Supplemental data:

VIPAR, a quantitative approach to 3D-histopathology applied to lymphatic malformations

René Hägerling[1], Dominik Drees[2], Aaron Scherzinger[2,3], Cathrin Dierkes[1], Silvia Martin-Almedina[4], Stefan Butz[5], Kristiana Gordon[4], Michael Schäfers[6,7], Klaus Hinrichs[3,7], Pia Ostergaard[4], Dietmar Vestweber[5], Tobias Goerge[8], Sahar Mansour[4], Xiaoyi Jiang[2,7], Peter S. Mortimer[4] and Friedemann Kiefer[1,6,7]

1. Max Planck Institute for Molecular Biomedicine, Mammalian Cell Signaling Laboratory, Röntgenstrasse 20, 48149 Münster, Germany
2. University of Münster, Department of Computer Science, Pattern Recognition and Image Analysis Group, Einsteinstrasse 62, 48149 Münster, Germany
3. University of Münster, Department of Computer Science, Visualization and Computer Graphics Group, Einsteinstrasse 62, 48149 Münster, Germany
4. Molecular and Clinical Sciences Institute, St George's University of London, Cranmer Terrace, London SW17 0RE, UK
5. Max Planck Institute for Molecular Biomedicine, Department Vascular Cell Biology, Röntgenstrasse 20, 48149 Münster, Germany
6. European Institute for Molecular Imaging (EIMI), University of Münster, Waldeyer Str. 15, 48149 Münster, Germany
7. DFG Cluster of Excellence 1003 'CiM – Cells in Motion', Münster, Germany
8. University Hospital of Münster, Department of Dermatology, Von-Esmarch-Strasse 58, 48149 Münster, Germany

Supplementary Figure 1: **Summary of the workflow for sample preparation, imaging and analysis using VIPAR.** (A) PFA-fixed skin biopsies comprising approx. 250 mm^3 tissue volume were wholemount immunostained to allow later visualization of the vascular systems by fluorescence microscopy. After completion of the staining procedure, samples were embedded in agarose and subsequently optically cleared with Murray's clear (benzyl alcohol:benzyl benzoate 1:2). (B) After completion of the clearing process, stacks of optical sections covering the entire sample volume were generated using a LaVision Biotec light-sheet microscope, UltraMicroscope II. (C) Digital 3D reconstruction was performed using the open source volume rendering framework Voreen, which was extended by an application specific user interface. (D) For automated image analysis and parameter quantification, newly generated analytical tools were applied, which allowed the automated extraction and quantitative analysis of vascular parameters from skin tissue volume reconstructions. The chart shows a pipeline overview of data acquisition (dark grey), processing (orange) and subsequent analysis (yellow) of blood and lymphatic vessels. After generation of image stacks depicting both vessel types, lymphatic vessels were segmented using a random walker segmentation approach (27), blood vessels by a hessian vesselness extraction (28) followed by thresholding. After post processing of the segmented vascular structures, the vascular trees were skeletonized (29, 30) and various features were extracted from the volume data and displayed either as whisker box plot or bar graph.

Supplemental Figure 1 - Hägerling et al.

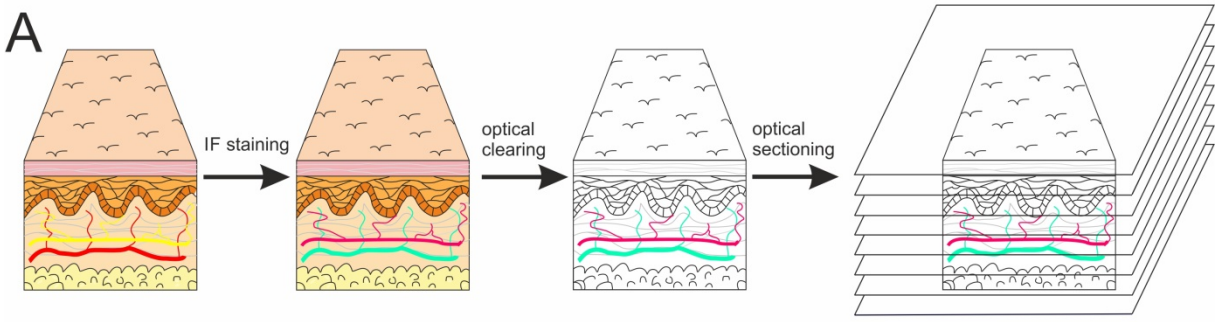

B

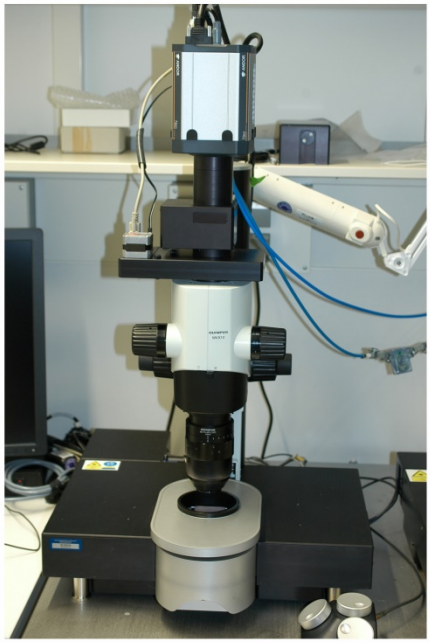

C

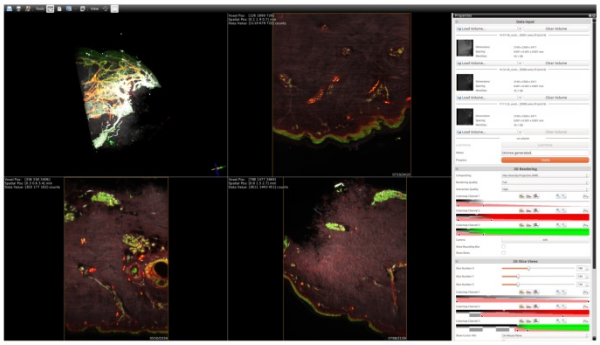

D

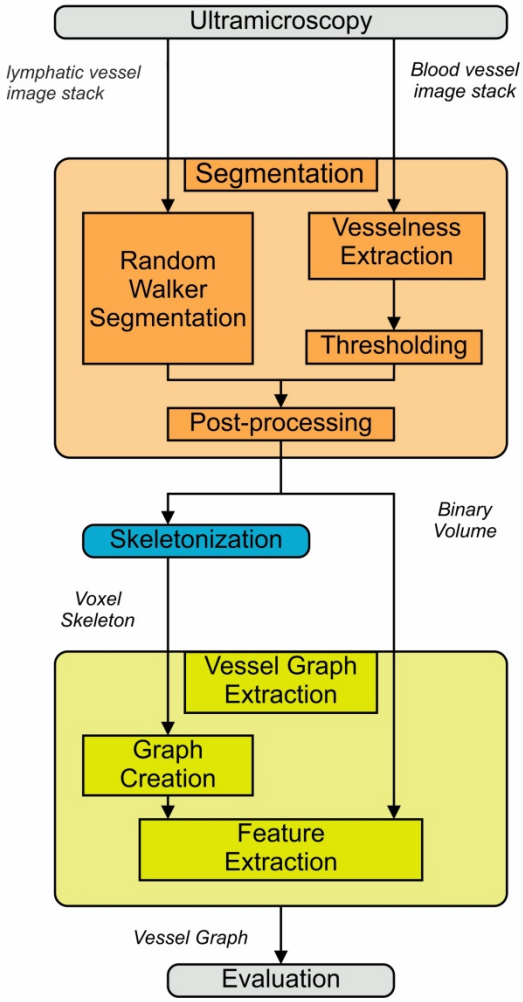

Supplementary Figure 2: **Clinical manifestations of a patient with WILD syndrome.** (A, B) Patient with WILD-Syndrome demonstrating multisegmental lymphoedema of upper and lower left limb. Note the vascular malformations on the chest (red arrow, A) as well as extensive epidermal naevi on the trunk of the patient (white arrow A). (C) Lymphoscintigraphy revealed an abnormally high lymphatic drainage in the right lower limb suggesting coexistent varicose veins. In contrast to the right extremities, the upper and lower left limbs show severely diminished lymphatic drainage. Left column values denote reduction of tracer activity at the injection site after 2 hours. Right column values indicate tracer uptake into inguinal and axillar lymph nodes two hours after tracer injection, reference uptake values are indicated in brackets. (D-F) Histology of a papillomatous, pedunculated lesion at the left foot of the patient revealed classical epidermal signs of lymphoedema (hyperkeratosis, parakeratosis, acanthosis), interstitial fluid accumulation in the dermis as well as increased collagen deposition. Of note, the number and diameter of lymphatic vessels are increased. Red dashed boxes in (D) are shown at higher magnification in E and F.

Supplemental Figure 2 - Hägerling et al.

A

B

C

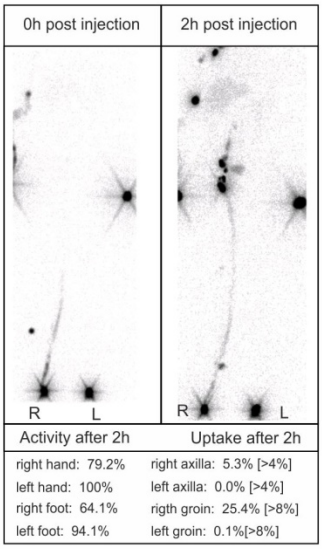

Activity after 2h		Uptake after 2h	
right hand:	79.2%	right axilla:	5.3% [>4%]
left hand:	100%	left axilla:	0.0% [>4%]
right foot:	64.1%	rigth groin:	25.4% [>8%]
left foot:	94.1%	left groin:	0.1%[>8%]

D

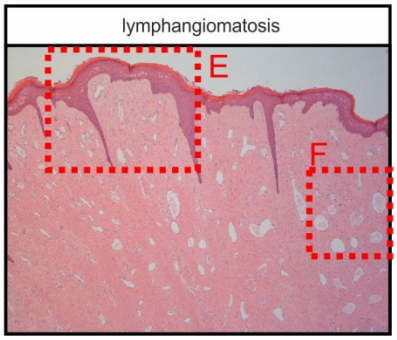

E

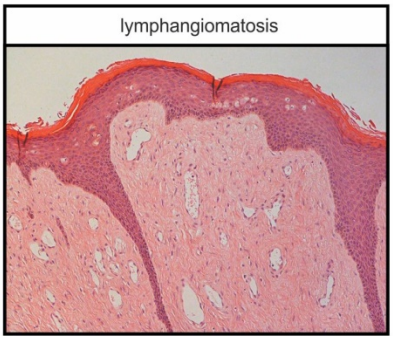

F

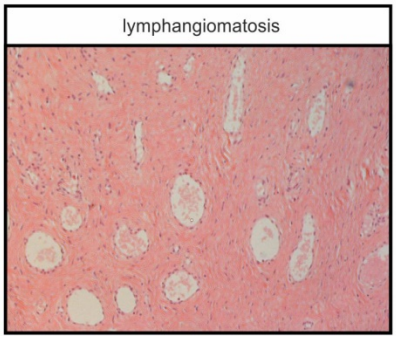

Supplementary Figure 3: **Description of the extracted vascular parameters.** (A) The shortest track between two nodes (black circles) is defined as *distance* (red line), the extracted skeletal length between two nodes as *length* (green line) and the ratio between distance and length as *straightness*. (B) Lymphatic vessels surfaces (grey) were defined by random walker segmentation.Subsequently determined skeletons, i.e. medial vessel axes, are represented by blue lines. Red circles denote branching points (nodes) in the skeleton. The abstract topological representation of the vessel network is exemplarily depicted using the red dashed line denoting a vessel segment between the two nodes. The vessel cross-section is marked in magenta. The cross-section describes the ratio of the volume enclosed and the length of the skeletonized vascular element. (C) Definition of the vascular parameters maximal radius (red), minimal radius (blue), average radius (green) and roundness. (D) Each vascular skeletal element is delimited by its distal branching points or skeletal nodes, which can be classified according to the numbers of segments that originate from a given node. If the number of their originating segments is unequal, the nodes of a particular segment can be classified into higher and lower degree nodes by the number of originating segments. Spherical vascular skeletal elements are classified as branching point degree zero, elonganted, non-connected elements as branching point degree one. It should be noted that branching points with connectivity of two, were not considered in this analysis as they do not represent an actual vessel node or branching point in the system.

Supplemental Figure 3- Hägerling et al.

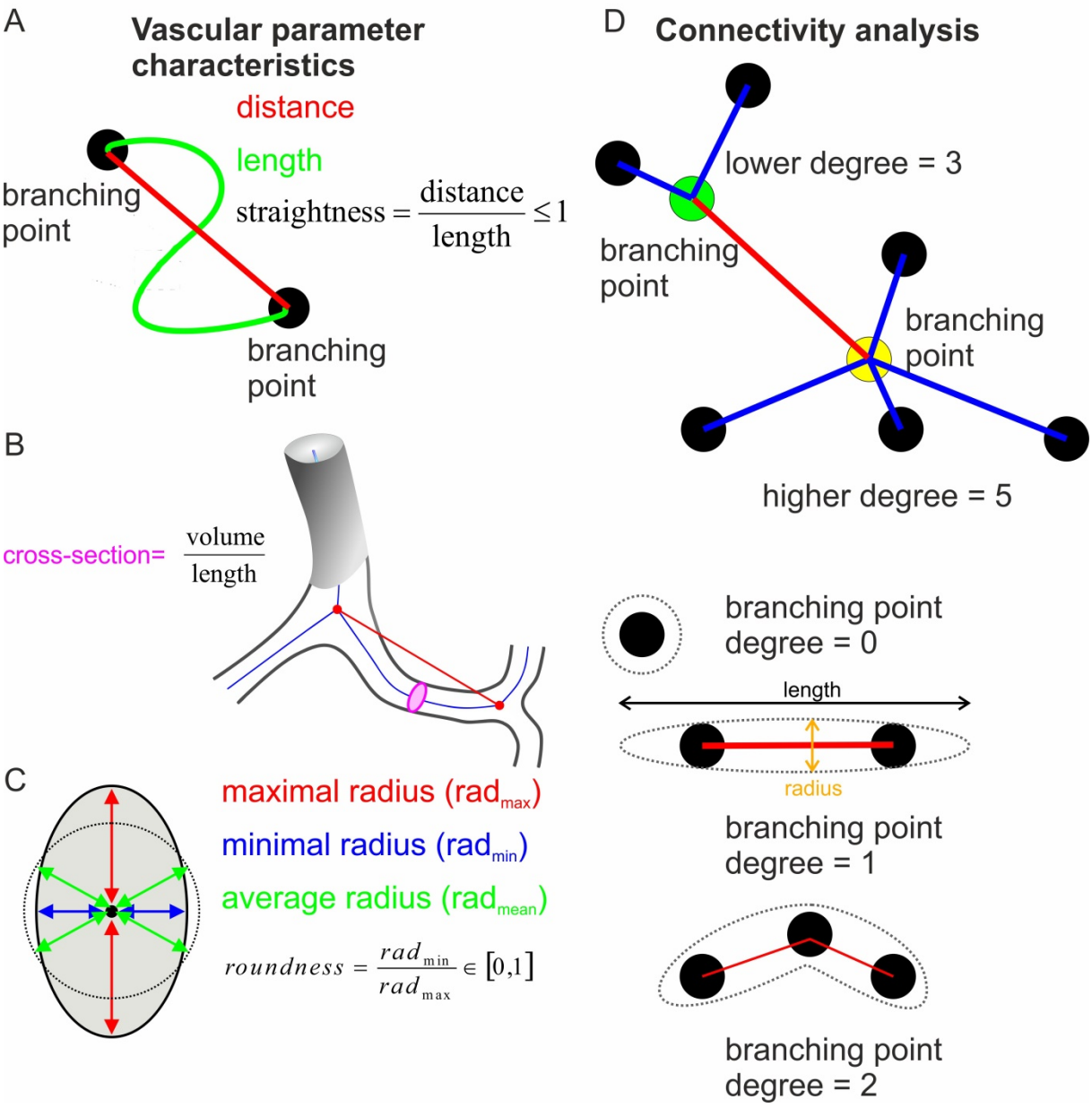

Supplementary Figure 4: **Correlation plot for automatically extracted vascular parameters**. Pearson's correlation coefficient was determined for the automatically extracted values of different vascular parameters. High correlation coefficients are indicated by bluish colour hues while low correlation values are indicated by reddish-white colour hues.

Supplemental Figure 4 - Hägerling et al.

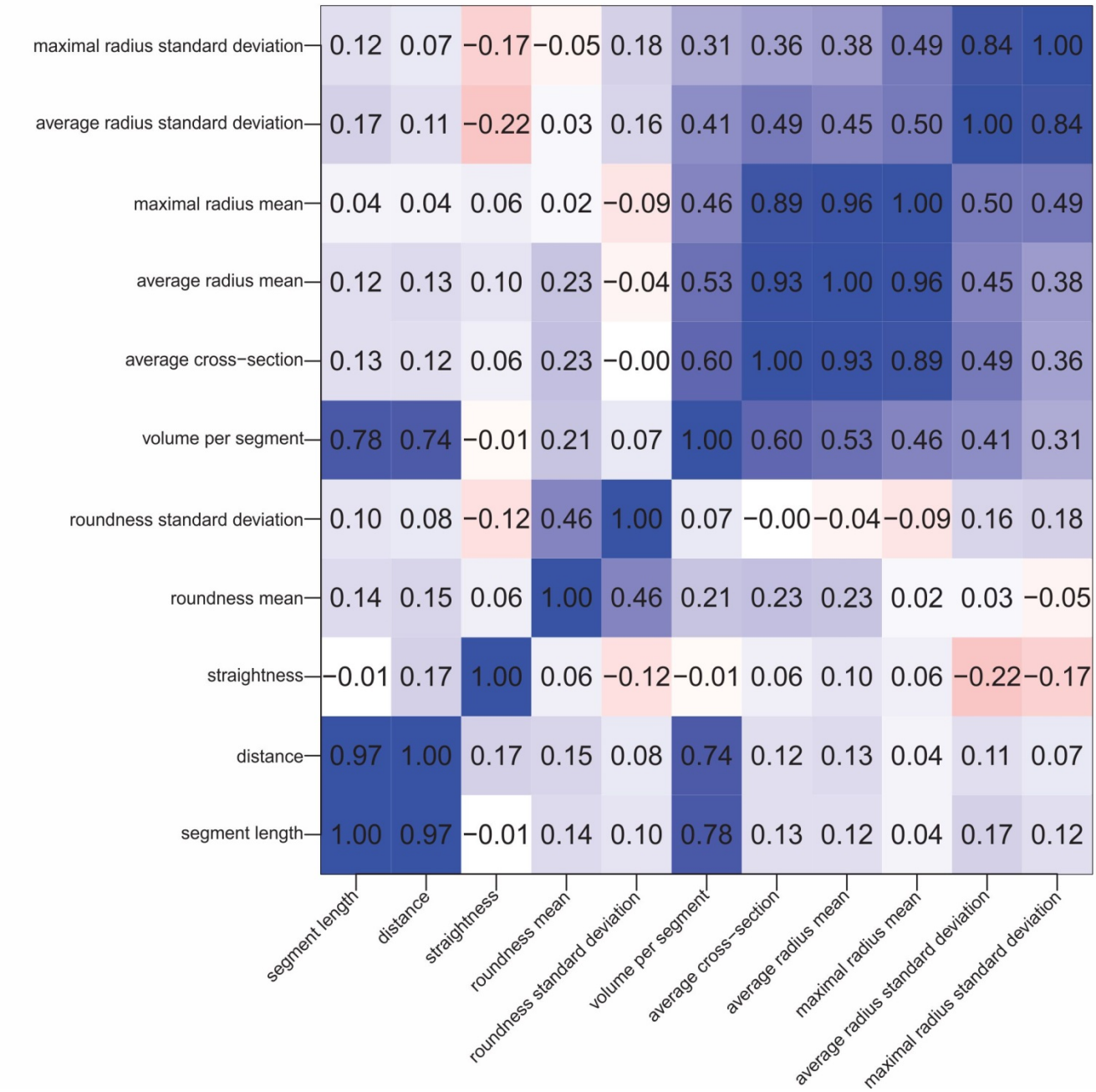

SUPPLEMENTARY VIDEOS

Supplementary Video 1: **3D reconstruction of a healthy skin biopsy revealing the vessel architecture of blood and lymphatic vessels**. A wholemount immunostained human skin biopsy was analysed using light sheet microscopy. Shown is a 3D reconstruction using the volume rendering package Voreen visualizing blood vessels (marked by ESAM1 staining, white) and lymphatic vessels (PDPN surface marker (red), PROX1 nuclei (green)). Areas of condensed PROX1 signal represent lymphatic valves.

Supplementary Video 2: **3D reconstruction of the lymphatic vasculature of a lymphoedematous skin biopsy elucidates disrupted and non-connected lumenised lymphatic vasculature.** Skin biopsy wholemount immunostained for PDPN (PODOPLANIN) was subjected to light sheet-based microscopy (UltraMicroscope II) and the obtained image stack was 3D reconstructed and visualized using the Voreen software package.

Supplementary Video 3: **3D reconstruction of the lymphatic vasculature of a lymphangiomatous skin biopsy reveals hyperplasia of disorganized lymphatic vessels.** A skin biopsy wholemount immunostained for PDPN (PODOPLANIN) was subjected to light sheet-based microscopy (UltraMicroscope II) and the obtained image stack was 3D reconstructed and visualized using the Voreen software package.